Astron. Astrophys. 329, 624–630 (1998)

ASTRONOMY AND ASTROPHYSICS

OSSE observations of the Orion giant molecular cloud during 1996

M.J. Harris[1], R.J. Murphy[2], G.H. Share[2], W.N. Johnson[2], R.L. Kinzer[2], J.D. Kurfess[2], and K. McNaron-Brown[3], and W.R. Purcell[4]

[1] USRA/GVSP, Code 661, NASA/Goddard Spaceflight Center, Greenbelt, MD 20771, USA
[2] Naval Research Laboratory, Code 7650, Washington DC 20375-5352, USA
[3] Physics/CSI, George Mason University, Fairfax, VA 22030, USA
[4] Dept. of Physics and Astronomy, Northwestern University, Evanston, IL 60208, USA

Received 12 December 1996 / Accepted 20 August 1997

Abstract. We have combined all OSSE spectra of the Orion molecular cloud complex obtained through the end of 1996 and searched them for evidence of cosmic-ray induced γ-ray lines in the 3–7 MeV energy range, as detected by COMPTEL (Bloemen et al. 1994, 1997). We do not detect any significant line emission; our flux estimate for broad-line emission of $1.5 \pm 1.0\ 10^{-4}\ \gamma/(\mathrm{cm}^2\text{-s})$ is consistent with the spatially-extended flux $1.3\ 10^{-4}\ \gamma/(\mathrm{cm}^2\text{-s})$ measured by Bloemen et al. (1997).

Key words: ISM: individual objects: Orion clouds – cosmic rays – gamma-rays: observations

1. Introduction

Bloemen et al. (1994) were the first to detect anomalous γ-ray emission from the Orion giant molecular cloud complex at energies 3–7 MeV, using data obtained by the COMPTEL instrument on board the *Compton* Observatory. They interpreted this emission as arising from the de-excitation of excited states in nuclei of ^{12}C (excitation energy 4.44 MeV) and ^{16}O (at 6.13 MeV). The lines appeared to be broadened by $\simeq$ 1 MeV, leading Bloemen et al. (1994) to suggest a kinematic effect: the ^{12}C and ^{16}O nuclei, having been accelerated to energies of tens of MeV, were excited by impacts on stationary target nuclei. De-excitation occurring in flight would naturally give rise to Doppler-broadened lines (Ramaty et al. 1979).

Bloemen et al. (1994) measured a rather weak flux $\sim 10^{-4}\ \gamma/(\mathrm{cm}^2\text{-s})$ in these lines, which explains why their existence has not yet been confirmed by any instrument other than COMPTEL (see below). As further COMPTEL observations have been made and analysed, several unexpected properties of the Orion emission have emerged. It was early recognized that Bloemen et al. (1994) ought to have detected lines in the 1–3 MeV range if several other species (e.g. ^{20}Ne) had been accelerated along with ^{12}C and ^{16}O in the expected solar-like proportion (Ramaty et al. 1995). The accelerated population must come from an environment heavily enriched in ^{12}C and ^{16}O only, such as a Wolf-Rayet star wind or core-collapse supernova (Bykov & Bloemen 1994). Second, the energy losses by ionization of the accelerated nuclei might produce a much higher infrared luminosity from the cloud complex than is measured (Cowsik & Friedlander 1995). Third, differential excitation of the magnetic sub-levels in the excited states of ^{12}C and ^{16}O ought to lead to anisotropic emission about the direction of motion, and so to Doppler splitting of the lines (Bykov et al. 1996). Finally, the emission from the Orion cloud seems relatively strong in comparison to that from the Galactic molecular clouds as a whole, which would follow the radio emission from CO. This is evident from the inability of Harris et al. (1995, 1996) to detect similar lines from the Galactic center in data from either *SMM* or OSSE.

Some of these issues were addressed in the most recent observations of the Orion lines, made by COMPTEL and reported by Bloemen et al. (1997). By including data obtained between 1994–1996, they were able to make a more sensitive measurement of the total line flux from the Orion region, amounting to $(1.28 \pm 0.15)\ 10^{-4}\ \gamma/(\mathrm{cm}^2\text{-s})$. A better spectrum of the γ-ray lines was measured, which shows weak evidence of the Doppler shifting and splitting expected from the kinematic arguments of Bykov et al. (1996). Bloemen et al. (1997) also obtained an improved image of the spatial distribution of the lines in the Orion region. The peaks in this distribution appear to fall in between the peaks of CO emission measured by Maddalena et al. (1986), which presumably trace the target mass for the accelerated particles. This small-scale anticorrelation could cause the energy deposition by the accelerated particles to be less than that expected by Cowsik & Friedlander (1995).

The γ-ray line emission from Orion detected by Bloemen et al. (1994, 1997) has not yet been confirmed by any instrument other than COMPTEL. A weak upper limit was obtained by

Send offprint requests to: M.J. Harris

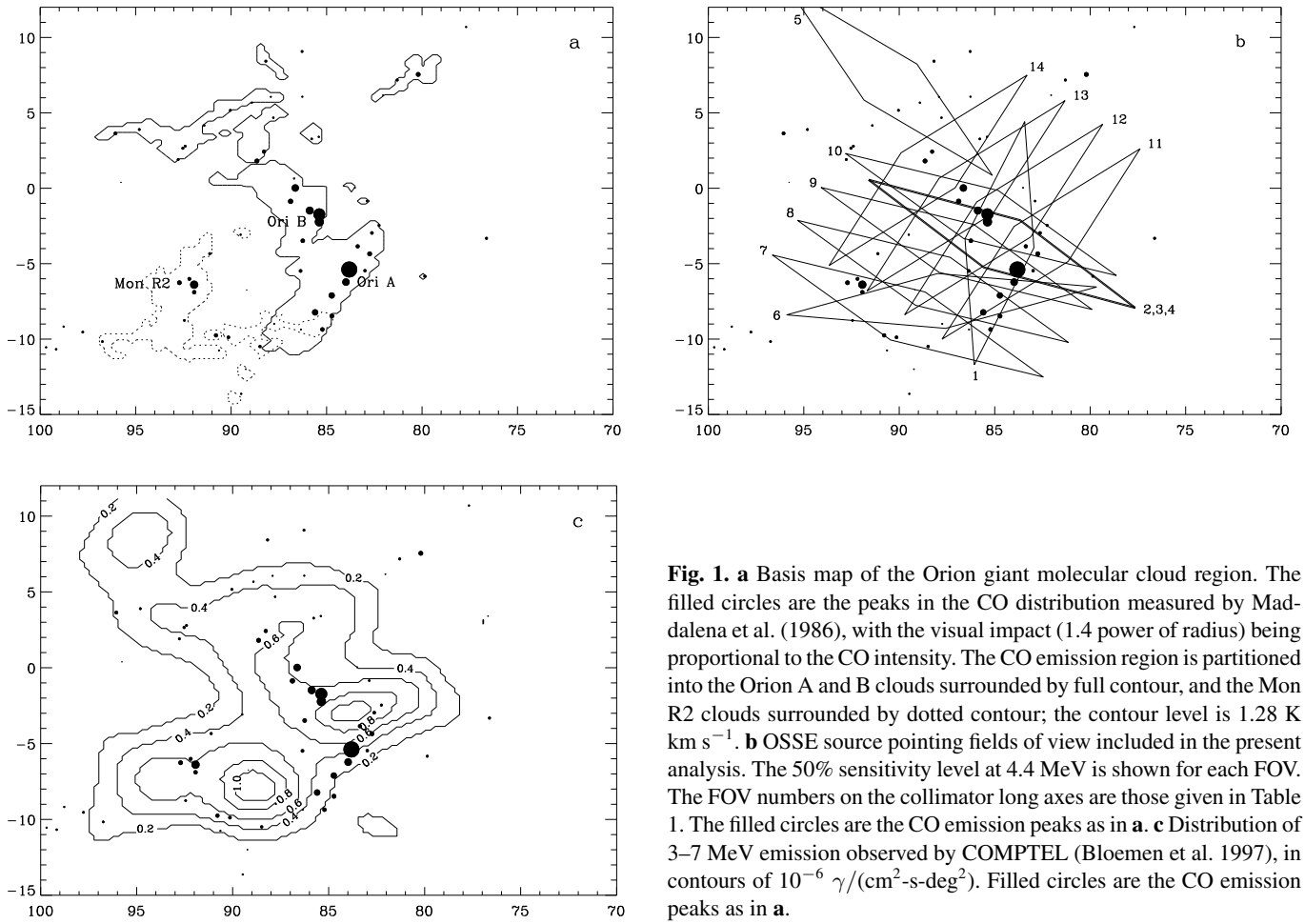

Fig. 1. a Basis map of the Orion giant molecular cloud region. The filled circles are the peaks in the CO distribution measured by Maddalena et al. (1986), with the visual impact (1.4 power of radius) being proportional to the CO intensity. The CO emission region is partitioned into the Orion A and B clouds surrounded by full contour, and the Mon R2 clouds surrounded by dotted contour; the contour level is 1.28 K km s^{-1}. **b** OSSE source pointing fields of view included in the present analysis. The 50% sensitivity level at 4.4 MeV is shown for each FOV. The FOV numbers on the collimator long axes are those given in Table 1. The filled circles are the CO emission peaks as in **a**. **c** Distribution of 3–7 MeV emission observed by COMPTEL (Bloemen et al. 1997), in contours of 10^{-6} $\gamma/(\mathrm{cm}^2\text{-s-deg}^2)$. Filled circles are the CO emission peaks as in **a**.

Harris et al. (1995) from *SMM* data, 3 10^{-4} $\gamma/(\mathrm{cm}^2\text{-s})$. A more sensitive measurement, covering only the central part of the molecular cloud complex, was made from OSSE data by Murphy et al. (1996). If the Bloemen et al. (1994) source had been point-like and midway between the CO emission peaks Orion A and Orion B, Murphy et al. (1996) would have detected it at a level $\sim 5\sigma$, whereas they in fact made no detection. It is clear that, as suggested by Bloemen et al. (1997), the emission comes from a region much larger than a single OSSE field of view (FOV). In the present work, we have combined the spectra from several OSSE FOVs in the Orion region obtained during 1996, together with those used by Murphy et al. (1996), amounting to 14 FOVs. The total OSSE exposure to the Orion region is approximately double that available to Murphy et al. (1996), and is much more uniformly distributed across the region. We can therefore provide further constraints on the spatial distribution of the line emission.

Models of the cosmic-ray interactions which produce the 4.4 and 6.1 MeV lines also predict a low level of line emission at 0.511 MeV, due to annihilation of positrons produced at the same time. Ramaty et al. (1995) estimate this line flux at $\sim$ 2 10^{-5} $\gamma/(\mathrm{cm}^2\text{-s})$. We searched in the same spectra for this line also.

2. Observations and analysis

2.1. Observations

A map of the CO emission from the Orion region appears in Fig. 1a. The CO peaks (Maddalena et al. 1986) are shown by filled circles, while the outer contours of the CO emission are shown by lines. There are in fact two quite distinct clouds in the Orion direction. The most intense sources, Orion A and B, are members of a cloud complex whose distance is 450 pc, while the nearby source Mon R2 is about twice as distant (830 pc: Xie & Goldsmith 1994). We refer to these complexes as "Orion" and "Monoceros", respectively, and we shall treat them separately throughout, since they are physically detached.

The OSSE FOVs which were used in our analysis are given in Table 1. Of these Viewing Periods (VPs), five were dedicated to the Orion complex (VPs 419.1, 419.5, 420, 522 and 523), and were as far as possible optimized for this purpose; however, VP 522 contained very little live time due to competition from a Target of Opportunity. The FOVs are shown relative to the CO distribution in Fig. 1b. It can be seen that, while almost all of the "Orion" region is covered in some degree, the exposure to the "Monoceros" region is meagre, given that FOVs 7 and 8 (VP 522) were deficient in live time and FOV 6 (VP 521) was not

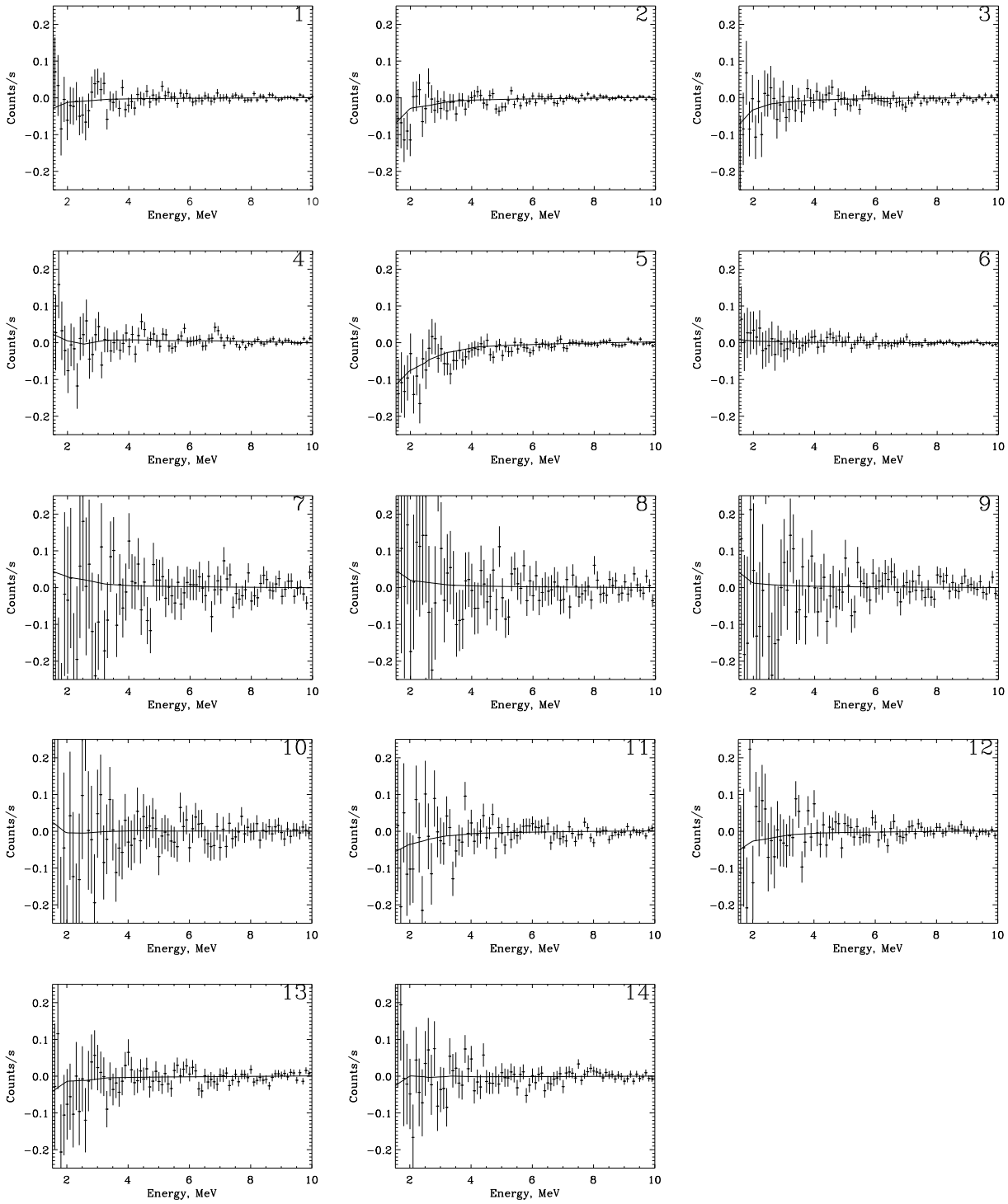

Fig. 2. 1–14 OSSE spectra from the 14 FOVs in Table 1 in the range 1.5–10 MeV. Data points are in 100 keV bins. Full lines – predicted background due to detector scan angle-dependent effects.

optimized for a Monoceros observation (the OSSE background pointings are in fact so close to FOV 6 that they largely overlap with the Mon R2 complex). Our measurements are therefore relevant mainly to the "Orion" region. Fortunately, the γ-ray line emission reported by COMPTEL is mainly from the "Orion" region, as shown in Fig. 1c, so that our FOVs are fairly well suited to a comparison of OSSE and COMPTEL results.

The spectra obtained in all 14 OSSE observations are shown in Fig. 2. Certain systematic effects are visible in these spectra. The OSSE instrument obtains spectra of a source during 2 min intervals, with one or more of its four detectors (Johnson et al. 1993), following which a background spectrum is generally taken by slewing the on-source detector(s) to an offset position for the next 2 min. It has been discovered that the background measurements vary systematically according to the distance between the offset positions, as a function of the on-source detector's scan angle position. In general, the effect is strongest when backgrounds are taken only on one side of the source, or when the offset positions are asymmetric about the source position. Table 1 shows that several of the VPs used in this study fall into these categories, with the worst case being FOV 5.

For typical background offset angles of a few degrees, the magnitude of the effect is $\sim$ 1% of the total count rate. This is comparable to the limiting sensitivity, and it is therefore of great importance to correct our observations for it, especially for weak sources. We have studied the dependence of the effect on detector, scan angle and energy using two different sets of data. The OSSE instrument team has observed a large sample of AGNs, using very many scan angle and detector combinations (see e.g. McNaron-Brown et al. 1995). The background offsets in this sample were small (typically 4.5°), but a wide variety of scan angles were sampled. A different set of observations was made of large areas towards Virgo and the South Galactic Pole, for survey purposes, which employed a large number of background offsets, ranging up to $\sim$ 20°. After correcting for the presence of known sources, the differences between count rates in each background-source pair were derived, as functions of detector, scan angle and energy.

The resulting systematics were found to be in all cases, to a first approximation, smooth functions of scan angle, constant with time, and devoid of spectral lines. We therefore used a sub-set of them as empirical correction factors for our measured spectra. To minimize any possible dependence on the overall background level, we derived the background correction only from data obtained subsequent to the reboost of the *Compton* Observatory in 1993 December to a higher altitude, since when the background has been relatively stable. The corrections were computed for the relevant detector and scan angle combinations used in our observations, and subtracted from the measured spectra. These correction factors, compared with the uncorrected data, are shown in Fig. 2 between 1.5–10 MeV. It is clear that in general the systematic continua in the data in Fig. 2 are very well predicted by the correction factors (solid lines), including the worst case (FOV 5, Fig. 2e).

Even after the removal of these systematics, the background-subtracted spectra still contain weak narrow systematic features of unknown origin. These features, previously noticed by Murphy et al. (1996), tend to be at lower energies ($\sim$ 2.5 MeV) than the lines in which we are interested. They do not appear to have any systematic effect on our analysis procedure (next section) except to increase the χ^2 of our fits slightly (Murphy et al. 1996).

2.2. Analysis

After correction for the detector scan angle dependence (previous section), none of our spectra show strong residual continua between 2–10 MeV. We fitted the corrected spectra using simplified spectral models of the line emission at 4.4 and 6.1 MeV seen by COMPTEL. These models were the same as those used by Murphy et al. (1996), namely two independent Gaussian lines at energies 4.44 and 6.13 MeV which may be either narrow (FWHM 95 and 110 keV respectively) or broad (FWHM 700 keV each). These models are also very similar to those employed by Harris et al. (1995, 1996) in line searches toward Orion and the Galactic center. The results are not sensitive to which spectral model is used so long as the lines are sufficiently broad. The fitting was performed by the standard OSSE technique, which involves forward-folding the parametrized model spectrum through the OSSE instrument response, comparing with the measured spectrum, and adjusting the model parameters until the best fit (measured by χ^2) is obtained. To search for the 0.511 MeV annihilation line, we fitted the same spectra between 0.05–4 MeV with the model spectrum of Purcell et al. (1993), which consists of a narrow line at 0.511 MeV, a continuum below 0.511 MeV due to annihilation via positronium formation, and an underlying power law.

Having measured the line strengths in each FOV in this way, we attempted to combine the results for different FOVs in order to constrain the spatial distribution of the emission. We adopted four possible model distributions and calculated the overlap between each distribution and the FOVs listed in Table 1 and plotted in Fig. 1b. Three of these distributions were illustrated in Fig. 1a and Fig. 1c, namely the CO emission mapped by Maddalena et al. (1986) from the separate regions of Orion and Monoceros, and the distribution of γ-ray line emission proposed by Bloemen et al. (1997). All of these distributions are sufficiently extended for OSSE background FOVs (Table 1) to cover part of them, so that any signal would be partly subtracted out. We attempted to gauge the seriousness of this problem by setting up a fourth, artificial distribution which would minimize this problem. The simplest such distribution is a uniform distribution covering only the target FOVs, excluding the backgrounds as far as possible — in essence, it is the union of the FOVs in Fig. 1b with small corrections for the background FOVs. We refer to this as the "maximized signal" distribution

A linear regression of the flux in each FOV against the relative exposure to each model distribution was performed, yielding a measurement of the flux from each distribution. We also investigated the possibility of a point source of the emission detected by COMPTEL and the accompanying 0.511 MeV line (next section).

Table 1. Fields of view observed by OSSE through the end of 1996.

Label, Fig. 1b	Viewing Period	Dates	Live time, s[a]	Center RA	Center Dec	Orientation[b]	Background offsets[c]
1	419.1	4/4/95–11/4/95	$3.80\ 10^5$	84.8	-3.6	-170.7	8.1,-7.2
2	419.5	9/5/95–23/5/95	$6.12\ 10^5$	84.6	-3.6	121.3	±12.0
3	420	23/5/95–6/6/95	$2.79\ 10^5$	84.6	-3.6	121.3	±12.0
4	420	23/5/95–6/6/95	$2.81\ 10^5$	84.6	-3.6	121.3	4.5,7.0
5	520	7/5/96–21/5/96	$2.97\ 10^5$	90.5	7.0	139.2	10.0,20.0
6	521	28/5/96–11/6/96	$4.75\ 10^5$	87.8	-7.5	83.5	±4.5
7	522	11/6/96–14/6/96	$2.49\ 10^4$	89.6	-8.5	119.7	-6.0,13.7
8	522	11/6/96–14/6/96	$2.68\ 10^4$	88.2	-6.2	119.7	-8.6,11.1
9	522	11/6/96–14/6/96	$3.03\ 10^4$	87.0	-4.0	119.7	-11.1,8.6
10	522	11/6/96–14/6/96	$3.03\ 10^4$	85.7	-1.7	119.7	-13.7,6.0
11	523	25/6/96–9/7/96	$1.12\ 10^5$	82.6	-3.7	39.4	-6.0,13.7
12	523	25/6/96–9/7/96	$1.07\ 10^5$	84.5	-2.1	39.4	-8.6,11.1
13	523	25/6/96–9/7/96	$1.19\ 10^5$	86.5	-0.5	39.4	-11.1,8.6
14	523	25/6/96–9/7/96	$1.19\ 10^5$	88.5	1.2	39.4	-13.7,6.0

[a] Total live time in all detctors on-source. All FOVs were observed by all 4 detectors, except 3 (detectors 1,2) and 4 (detectors 3,4).
[b] Long axis of collimator in degrees clockwise from celestial North.
[c] In degrees, positive toward celestial North.

Table 2. Line fluxes in 10^{-5} $\gamma/(\mathrm{cm}^2\text{-s})$ inferred for the Orion and Monoceros distributions of Fig. 1a, the COMPTEL distribution of Fig. 1c, and the "maximized signal" distribution of Fig. 1b.

Line	Distribution			
	Orion	Monoceros	COMPTEL	"max. signal"
Narrow 4.4 MeV	5.8 ± 3.8	6.6 ± 10.5	8.0 ± 5.2	2.7 ± 1.6
Narrow 6.1 MeV	0.8 ± 2.8	-3.2 ± 7.6	-1.1 ± 3.9	-0.1 ± 1.2
Total narrow	6.6 ± 4.7	3.5 ± 13.0	6.9 ± 6.5	2.7 ± 2.1
Broad 4.4 MeV	7.0 ± 6.0	22.4 ± 15.4	12.9 ± 8.2	4.4 ± 2.6
Broad 6.1 MeV	3.1 ± 3.9	3.0 ± 9.7	1.7 ± 5.4	1.2 ± 1.8
Total broad	10.1 ± 7.2	25.4 ± 18.2	14.6 ± 9.8	5.6 ± 3.2
Narrow 0.511 MeV	-5.0 ± 7.0	-11.6 ± 17.3	-6.9 ± 9.5	-3.8 ± 3.3

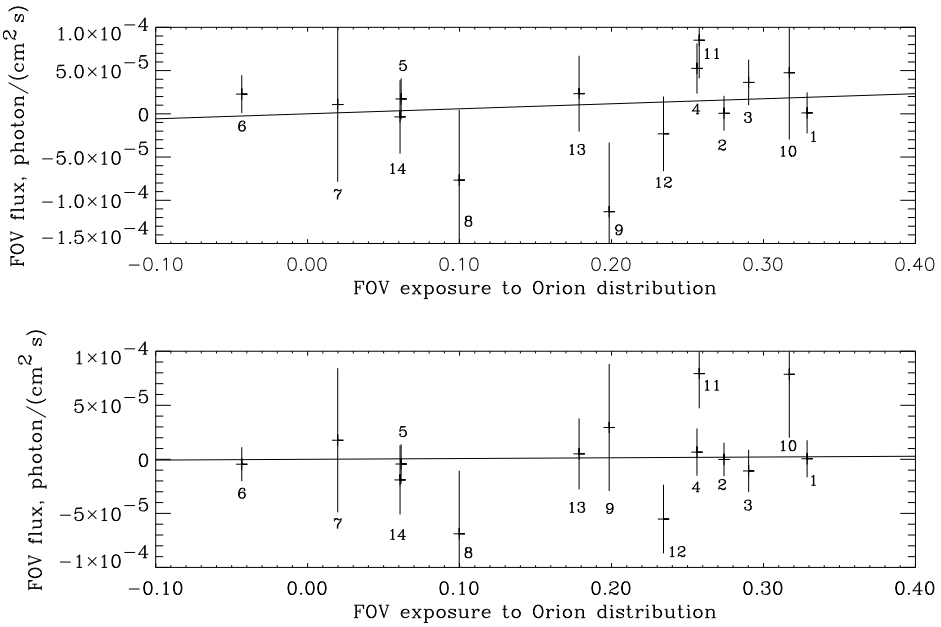

Fig. 3. Measured 4.44 MeV (top) and 6.13 MeV (bottom) narrow line fluxes in the FOVs of Fig. 1b, plotted against exposure of the FOV to the Orion distribution of Fig. 1a, corrected for background pointings.

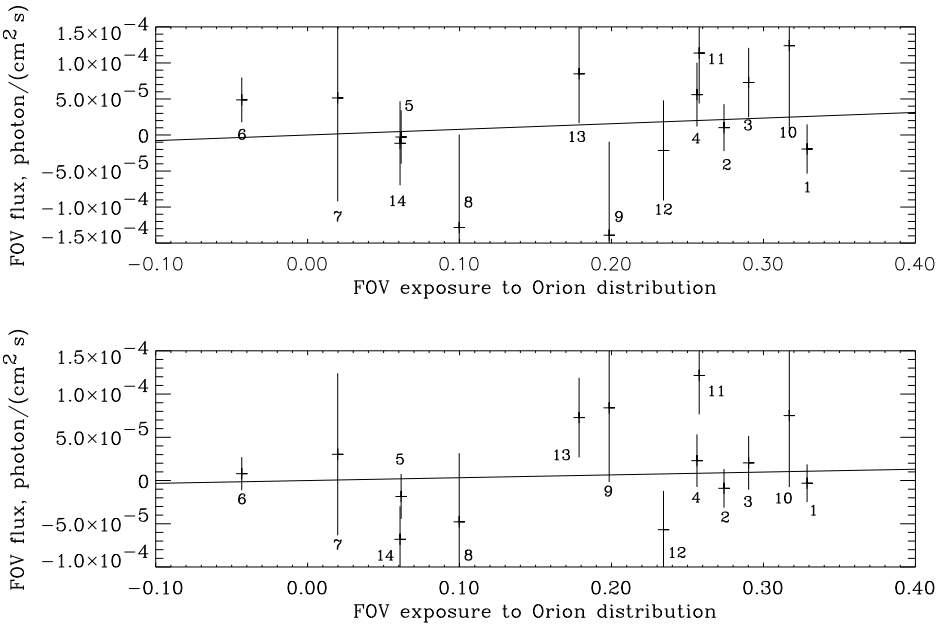

Fig. 4. Fluxes of broad 4.44 and 6.13 MeV lines, as in Fig. 3.

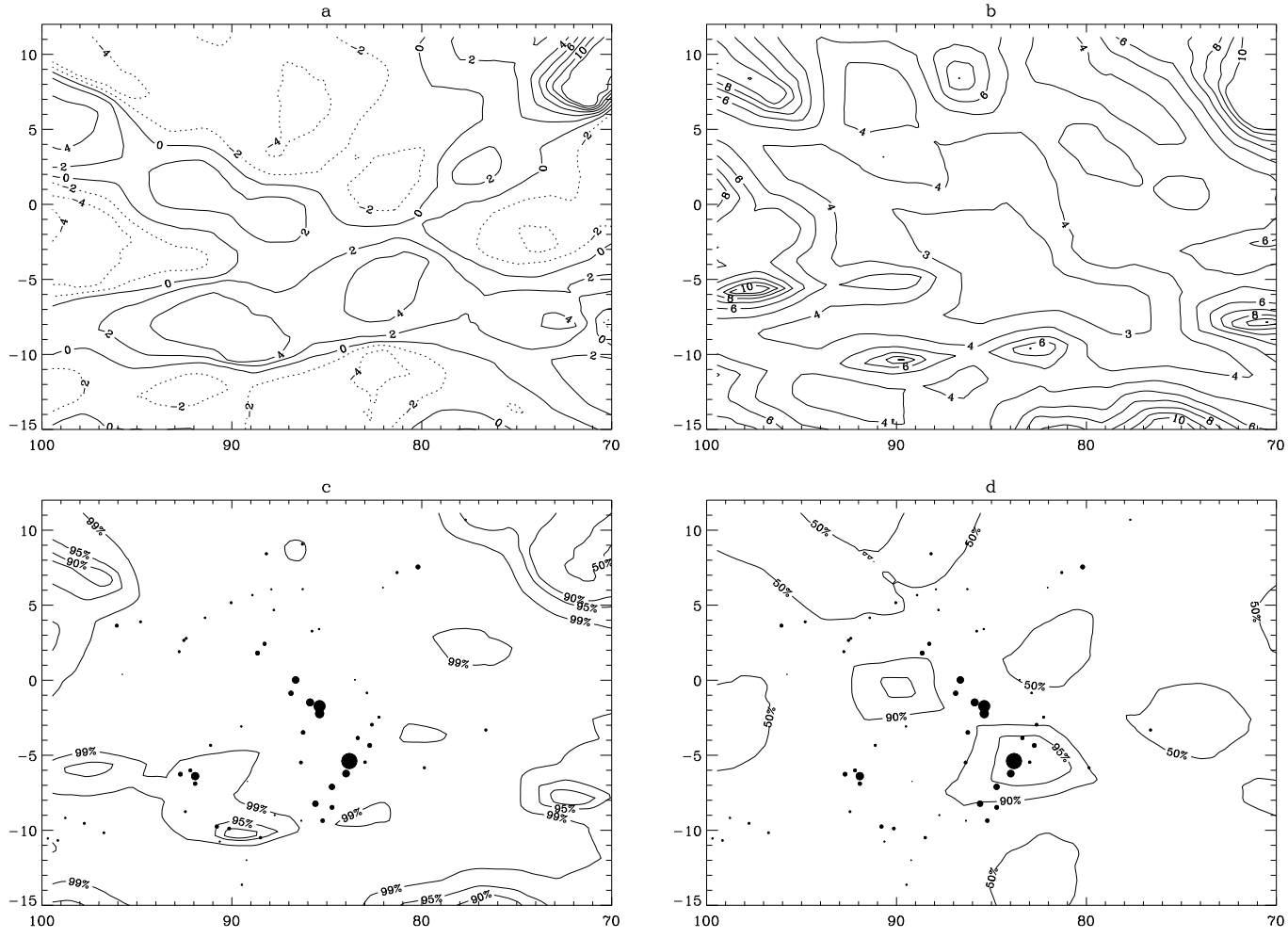

Fig. 5. a Point source fluxes necessary to explain our FOV measurements of the total broad 4.4 and 6.1 MeV lines, in units of 10^{-5} $\gamma/(\mathrm{cm}^2\text{-s})$. **b** Uncertainties in the point source fluxes in Fig. 5a, in units of 10^{-5} $\gamma/(\mathrm{cm}^2\text{-s})$. **c** Contours of the confidence with which a point source of broad 4.4 and 6.1 MeV line radiation at the COMPTEL level 1.28 10^{-4} $\gamma/(\mathrm{cm}^2\text{-s})$ can be excluded by our measurements. **d** Contours of the confidence with which a point source of 0.511 MeV line radiation at the predicted level ~ 2 10^{-5} $\gamma/(\mathrm{cm}^2\text{-s})$ can be excluded by our measurements.

3. Results and discussion

None of the observations listed in Table 1 yielded a significant positive flux in either narrow or broad γ-ray lines. In Figs. 3 and 4 we present the results of the measurements from all 14 OSSE FOVs, as a function of FOV exposure to the Orion cloud defined in Fig. 1a. There is no clearly significant trend of any line with exposure to Orion; the implied fluxes from the entire distribution (abscissa= 1.0) are $(6.6 \pm 4.7)\ 10^{-5}\ \gamma/(\mathrm{cm}^2\text{-s})$ (sum narrow lines) and $(10.1 \pm 7.2)\ 10^{-5}\ \gamma/(\mathrm{cm}^2\text{-s})$ (sum broad lines). The results for the other spatial models are given in Table 2; it is clear that the exposure of our FOVs to the Monoceros region is very poor, leading to large errors and measurements of little value. Our measurement of the total broad-line emission from the COMPTEL distribution, $(1.5 \pm 1.0)\ 10^{-4}\ \gamma/(\mathrm{cm}^2\text{-s})$, may be compared directly with the Bloemen et al. (1997) measurement $(1.28 \pm 0.15)\ 10^{-4}\ \gamma/(\mathrm{cm}^2\text{-s})$. Comparing the significance of this result with that for our "maximized signal" distribution, the difference is small (1.8σ versus 1.5σ). Thus the systematic error by which our flux measurements are underestimated due to subtraction of signal in background is probably $\leq 20\%$.

Our measurements are clearly more sensitive for narrow lines than for broad lines, as expected. Murphy et al. (1996) concluded that, for the small area around Orion A and B (center of our FOVs 1–4), a narrow line source could be excluded as the explanation of the observed COMPTEL flux at the 3.5σ level. We are able to extend that conclusion to the Orion region as a whole. Our result for the combined narrow lines, $(6.6 \pm 4.7)\ 10^{-5}\ \gamma/(\mathrm{cm}^2\text{-s})$, is incompatible with the total COMPTEL flux, if coming from the same (Orion) region, at the 90% level. Our measurement is not sensitive enough to exclude a narrow line source which is offset from Orion (as is Monoceros) or which is of larger extent (as is the observed COMPTEL emission).

Our broad line model is closer to the spectrum reported by COMPTEL (Sect. 1). However, our results for broad lines are less sensitive (Table 2), and do not contain sufficient information to generate a map comparable to that of Bloemen et al. (1997; our Fig. 1c). Just as we could only constrain the most extreme spectral energy distribution (narrow lines, as above), so we can constrain the narrowest possible spatial distribution, namely a point source. This is done by constructing a $\frac{1}{4}^\circ \times \frac{1}{4}^\circ$ grid and simulating the effect of a point source at each grid point upon the OSSE FOVs in Fig. 1b. At each point we determine the flux which best fits the sum of the measurements in all the OSSE FOVs which overlap the point.

In Fig. 5a we give the resulting point source fluxes, and in Fig. 5b the uncertainties on them, in the form of contours. As would be expected from the generally null FOV measurements, there are no grid points where a significant positive flux is required to explain our results. We compare each point flux with the total measured by COMPTEL from the whole area, $1.28\ 10^{-4}\ \gamma/(\mathrm{cm}^2\text{-s})$. The fluxes and uncertainties at almost every point fall well below this value, indicating that our measurements exclude a single point source for the whole COMPTEL emission from almost the whole region. This conclusion is expressed quantitatively in Fig. 5c. From each value in Figs. 5a and 5b we determine the discrepancy in standard deviations of a value $1.28\ 10^{-4}\ \gamma/(\mathrm{cm}^2\text{-s})$, which we then convert into a probability assuming a normal error distribution, i.e. the probability with which a point source of the entire COMPTEL emission can be excluded. We conclude that a point source of the COMPTEL emission can be ruled out at the 95% level almost everywhere in the region, and at the 99% level everywhere except the "Monoceros" region, and a few small areas west of the "Orion" region, as defined in Fig. 1a.

Our results for the narrow 0.511 MeV line were obtained in the same ways, and are presented in Table 2 and Fig. 5d. It is clear from Table 2 that they do not provide any constraints on diffuse sources of this line at the expected level $\sim\ 2\ 10^{-5}\ \gamma/(\mathrm{cm}^2\text{-s})$. However, point sources of 0.511 MeV radiation can be excluded for some regions. This is shown in Fig. 5d in the same way as in Fig. 5c, i.e. as contours of the probability with which a point source can be excluded. We see that this is the case at the $\geq 90\%$ level for the central region of "Orion" around Orion A, and for a small region north-east of it.

Acknowledgements. We are grateful to Dr. Loredana Bassani for permission to use the OSSE spectra from VP 521, and to Dr. Hans Bloemen for informing us of COMPTEL's most recent results before publication. This work was supported under NASA grant DPR S-67026F.

References

Bloemen, H., Wijnands, R., Bennett, K., et al. 1994, A&A 281, L5.
Bloemen, H., Bykov, A. M., Bozhokin, S. V., et al. 1997, ApJ, 475, L25.
Bykov, A. M., & Bloemen, H. 1994, A&A, 283, L1.
Bykov, A. M., Bozhokin, S. V., & Bloemen, H. 1996, A&A, 307, L37.
Cowsik, R. & Friedlander, M. W. 1995, ApJ, 444, L29.
Harris, M. J., Share, G.H., & Messina, D.C. 1995, ApJ, 448, 157.
Harris, M. J., Purcell, W. R., Grabelsky, D. A., et al. 1996, A&AS, 120, 343.
Johnson, W. N., Kinzer, R. L., Kurfess, J. D., et al. 1993, ApJS, 86, 693.
Maddalena, R. J., Morris, M., Moscowitz, J., & Thaddeus, P. 1986, ApJ, 303, 375.
McNaron-Brown, K., Johnson, W. N., Jung, G. V., et al. 1995, ApJ, 451, 575.
Murphy, R. J., Share, G. H., Grove, J. E., et al. 1996, ApJ, 473, 990.
Purcell, W. R., Grabelsky, D. A., Ulmer, M. P., et al. 1993, ApJ, 413, L85.
Ramaty, R., Kozlovsky, B., & Lingenfelter, R.E. 1979, ApJS, 40, 487.
Ramaty, R., Kozlovsky, B., & Lingenfelter, R.E. 1995, ApJ, 438, L21.
Xie, T., & Goldsmith, P. F. 1994, ApJ, 430, 252.

This article was processed by the author using Springer-Verlag LaTeX A&A style file *L-AA* version 3.